*ФИЗИКА ЭЛЕМЕНТАРНЫХ ЧАСТИЦ И АТОМНОГО ЯДРА*
*2013. Т. 44. ВЫП. 6*

# SPIN POLARIZED $^3$He: FROM BASIC RESEARCH TO MEDICAL APPLICATIONS

*S. Karpuk* [1,*], *F. Allmendinger* [2], *M. Burghoff* [3], *C. Gemmel* [1], *M. Güldner* [1], *W. Heil* [1], *W. Kilian* [3], *S. Knappe-Grüneberg* [3], *Ch. Mrozik* [1], *W. Müller* [3], *E.W. Otten* [1], *M. Repetto* [1], *Z. Salhi* [1], *U. Schmidt* [2], *A. Schnabel* [3], *F. Seifert* [3], *Yu. Sobolev* [1], *L. Trahms* [3], *K. Tullney* [1]

[1] Universität Mainz, Institut für Physik, Mainz, Germany

[2] Universität Heidelberg, Physikalisches Institut, Heidelberg, Germany

[3] Physikalisch-Technische Bundesanstalt, Berlin, Germany

Polarization of $^3$He gas by means of optical pumping is well known since the early 1960s with first applications in fundamental physics. Some thirty years later it was discovered that one can use hyperpolarized $^3$He as contrast agent for magnetic resonance imaging of the lung. The wide interest in this new method made it necessary to find ways of polarizing $^3$He in large quantities with high polarization degrees. A high performance polarizing facility has been developed at the University of Mainz, designed for centralized production of hyperpolarized $^3$He gas. We present the Mainz concept as well as some examples of numerous applications of spin polarized $^3$He in fundamental research and medical applications.

PACS: 06.30.Ft; 11.30.Cp; 11.30.Er; 14.80.Va; 25.55.Ci; 32.30.Dx; 32.80.Xx; 87.61.-c

## INTRODUCTION

Since 1963, it is known that $^3$He gas can be spin polarized by means of optical pumping techniques [1]. Optical pumping transfers polarization from photons to atoms by resonant absorption of circularly polarized light. In spin exchange optical pumping (SEOP), angular momentum from a circularly polarized laser beam is indirectly transferred to the $^3$He nuclei via alkali metal atoms (usually rubidium). A second method to polarize $^3$He gas is metastability exchange optical pumping (MEOP) with direct transfer of angular momentum from resonant laser light to $^3$He atoms. Each technique has its own advantages and limitations. For

*Corresponding author: E-mail: karpuk@uni-mainz.de

instance, SEOP directly operates at high pressure but is a relatively slow process, while MEOP is a much faster process, but only operates at low pressures of about 1 mb and usually requires mechanical compression for later applications. In MEOP only a small fraction of metastable $^3$He atoms is produced in a low pressure gas discharge. These metastable helium atoms can absorb resonant pump light at 1083 nm and be optically pumped. For the $^3$He isotope in the excited metastable state, the efficient hyperfine coupling between the nucleus and the electrons results in an almost instantaneous transfer of angular momentum into the nuclear system. This nuclear orientation is again rapidly transferred to the $^3$He ground state atoms by the so-called metastability exchange collisions [2].

The necessity of providing polarized $^3$He gas in large quantities was originally demanded by nuclear physics experiments, where nuclear spin-polarized $^3$He was needed as a target for polarized neutrons: the spin of the polarized $^3$He is essentially carried by the spin of the bound neutron [3]. This property is used, for example, at the MAinz MIcrotron (MAMI) to extract the electric form factor of the neutron $G_{e,n}$ via a double polarized electron scattering experiment of type $^3\vec{\mathrm{H}}e\,(\vec{e}, e'n)$ [4]. The polarized $^3$He target was also used at the real photon beam at MAMI to investigate the Gerasimov–Drell–Hearn sum rule for the neutron [5].

Furthermore, the strongly spin-dependent capture cross section of neutrons from reactors and spallation sources in polarized $^3$He opens up the possibility of polarizing these neutrons over their full kinematical range from cold, thermal to hot neutrons [6]. Nowadays, polarized neutron scattering techniques are an indispensable and highly requested tool for studying magnetic phenomena in condensed matter physics [7].

In 1994, it was discovered that one can use spin polarized gases as contrast agent for magnetic resonance imaging (MRI) of the lung [8]. Soon after, research teams in the US and in Mainz/Heidelberg in Germany demonstrated the possibility to image human lungs using inhaled hyperpolarized $^3$He [9]. Spin-density distributions in the human lungs can be recorded during breath hold with high resolution. In addition, the MRI acquisition sequences can be made fast enough to provide dynamical ventilation data. Mapping physical parameters such as local relaxation times or apparent diffusion coefficients indirectly provide information on lung functioning or may reveal subtle changes in the alveolar region of the airways. It is generally recognized, that this imaging method has an unprecedented potential for morphological and functional analysis of the lung [10–12].

## 1. MAINZ POLARIZING FACILITY

The wide interest in $^3$He-MRI made it necessary to find ways of polarizing $^3$He in large quantities with high polarization degrees. In addition, storage, transport, and administration of hyperpolarized (HP) $^3$He as well as recovery of this rare helium isotope became important issues in assessing and spreading

this new, noninvasive diagnostic tool in medical research. A high performance polarizer unit has been developed in Mainz almost a decade ago [13]. Our concept of HP $^3$He production and delivery includes a remote type of operation, where the $^3$He is spin polarized at a central production facility from where it is transported to the potential users. After gas administration, the gas can be recovered and reused. The apparatus in Mainz is based on MEOP. The whole equipment is located in a homogeneous magnetic field of about 1 mT, which serves as a holding field for the spin polarized $^3$He nuclei (Figure). The apparatus essentially consists of three parts: the first part comprises the $^3$He reservoir and getters for gas purification. The second part is the optical pumping (OP) volume with its five cylindrical pumping cells, filled with $^3$He at about 1 mb. For optical pumping two 15 W fibre lasers at 1083 nm are used. The light is circularly polarized and is absorbed by the metastable atoms. The OP cells have a length of 2.4 m, each. In order to maximize light absorption, the laser light is back-reflected by means of dichroic mirrors so that it passes each OP cell twice. The nuclear polarization of the $^3$He gas can be monitored during the OP process by measuring the circular polarization of the 668 nm fluorescence light emitted during gas discharge. The third part contains the nonmagnetic, polarization-conserving piston compressor, driven by hydraulics in order to obtain gas pressures up to 5.0 b. In the first compression cycle, the hyperpolarized gas is compressed into a buffer cell of $V = 6$ l up to the pressures of 0.1–0.6 b, typically. In the second step, this gas is expanded into the stroke-volume ($V \sim 15$ l) of the compressor and recompressed in one cycle into a detachable transport cell. A polarization of 75 to 78% can be obtained at a production rate of about 1 standard liter per hour. These are the

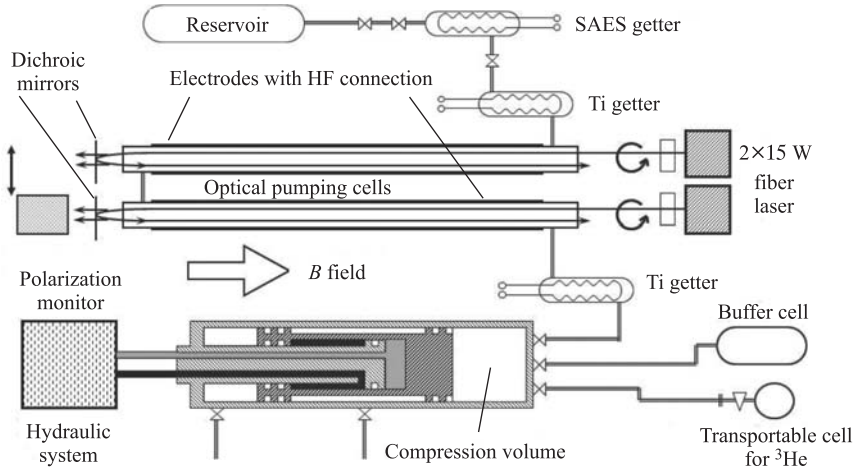


Sketch of the Mainz $^3$He polarizer. For further explanations, see the text

operation conditions, when the gas is used for fundamental physics applications, where high polarization degrees are demanded. For medical applications, where higher production rates are required, lower polarization values around 65% are sufficient. Here we work at a production rate between 2 and 3 standard liters per hour [13].

The HP $^3$He is stored and transported in relaxation-poor glass vessels, which are blown from GE180 glass. Without internal coating, longitudinal relaxation times $T_1$ of up to 250 h are reached [14]. That is sufficient for shipping the HP gas all around the world using specially designed transport units, which provide a homogeneous magnetic field of about 0.8 mT to guide the spins. The relative field gradient inside the cylindrical shaped transport boxes is about $1 \cdot 10^{-3}/\mathrm{cm}^{-1}$, where permanent magnets in combination with $\mu$-metal shields are used to provide that field homogeneity. The field gradient induced relaxation time at 2.7 b gas pressure was measured to be 400 h. In total, three spherical glass vessels of $V = 1.1$ l each, i.e., a total amount of HP gas of $\sim 9$ standard liters, can be shipped [15].

In order to administer the HP gas to patients or volunteers with high reproducibility and reliability, a new gas applicator unit has been built [16]. The patient's inspiratory and expiratory airflows are monitored during the whole experiments. The exhaled air/$^3$He mixture is collected into a He-tight bag and then compressed by means of a commercial diving compressor into a stainless steel bottle. The new administration unit fulfils the obligations given by Medical Devices Law and does not reduce the quality of MR imaging.

After usage, the $^3$He can be recovered in a gas purification unit — a combination of $LN_2$ trap, zeolith traps and a cold trap (8 K) [17]. The latter one is necessary to freeze out neon. The apparatus is able to separate helium from batches of up to 600 standard liters of helium/air mixture ($\sim 1 : 100$) with an efficiency of 95%. The gas purity reaches the specifications of commercial $^3$He gas from the supplier and can directly be reused for MEOP. We achieve a total recovery efficiency of about 80% for the whole $^3$He cycle, i.e., the losses per MRI application are reduced by a factor of 5.

In addition, a new, compact MEOP polarizer is being developed [18]. Contrary to our present apparatus, which serves as central polarizing facility, the compact polarizer is designed to serve as local polarizing facility for both basic research and medical applications. The decisive reduction in size is achieved by a new arrangement of the optical and mechanical components inside a specially designed magnetic shield that provides a very homogeneous field inside stretching across the entire coil volume.

All components of the HP $^3$He cycle have been optimized and are well established, now. The manufacturing authorization for human studies has been given for the production of HP $^3$He and the gas recovery [19]. This infrastructure has supported clinical research on lung imaging with HP $^3$He MRI worldwide and,

in particular, within the European networks PHIL (Polarized Helium to Image the Lung, 2000–2004, http://www.phil.ens.fr/frameset.html) and PHeLINet (Polarized Helium Lung Imaging Network, 2007–2011, http://www.phelinet.eu/).

## 2. TESTING FUNDAMENTAL SYMMETRIES IN $^3$He/$^{129}$Xe CLOCK COMPARISON EXPERIMENTS

The most precise tests of new physics are often realized in differential experiments that compare the transition frequencies of two co-located clocks, typically radiating on their Zeeman or hyperfine transitions. An essential assumption in this so-called clock comparison experiments is that the anomalous field $\mathbf{a}$, one is looking for, does not couple to magnetic moments but directly to the sample spins $\boldsymbol{\sigma}$. This direct coupling allows co-magnetometry that uses two different spin species to distinguish between a normal magnetic field and an anomalous field coupling. The advantage of differential measurements is that they render the experiment insensitive to common systematic effects, such as uniform magnetic field fluctuations.

In spite of the incredibly high relative accuracy of frequency determination ($\delta\nu/\nu = 3 \cdot 10^{-16}$ [20]), the absolute accuracy of a cesium atomic clock is reaching 3 $\mu$Hz under optimum conditions. To address fundamental questions in physics often associated with the experimental search for violation of fundamental symmetries in nature, much smaller frequencies or frequency shifts have to be traced. From that point of view, it is more appropriate to develop a clock that oscillates at low frequencies ($\sim$ 10 Hz), but shows the similar relative accuracy as a Cs atomic clock. Thus, frequency shifts in the pHz range caused by hypothetical interaction potentials might be accessible [21].

$^3$He/$^{129}$Xe clock comparison experiments based on free spin precession can be used as ultra-sensitive probe for nonmagnetic spin interactions of type

$$V_{\mathrm{nonmagn}} = \mathbf{a} \cdot \boldsymbol{\sigma}, \tag{1}$$

to study fundamental symmetries such as

a) Lorentz-violating signatures by monitoring, e.g., the relative Larmor frequencies or phases of the co-located $^3$He and $^{129}$Xe spin samples as the laboratory reference frame rotates with respect to a hypothetical background field with magnitude $\langle\tilde{b}\rangle$ and direction $\hat{\varepsilon}$ [22]:

$$\frac{V(r)}{\hbar} = \langle\tilde{b}\rangle\, \hat{\varepsilon}\frac{\boldsymbol{\sigma}}{\hbar}; \tag{2}$$

b) spin-dependent short-range interactions induced by light, pseudoscalar particles, like the axion (CP violation) [23]:

$$\frac{V(r)}{\hbar} = c\boldsymbol{\sigma}\frac{\hat{r}}{\hbar}, \tag{3}$$

where $\hat{r}$ is the unit displacement vector from the polarized bound neutron (according to the Schmidt model [24]) to the unpolarized nucleon of the matter samples as well as

c) the search for an electric dipole moment of $^{129}$Xe (CP-violation) [25]:

$$\frac{V(r)}{\hbar} = -|d_{\mathrm{Xe}}|\,\boldsymbol{\sigma}\frac{\mathbf{E}}{\hbar}, \tag{4}$$

where $\mathbf{E}$ is the electric field.

The observable to trace possible tiny nonmagnetic spin interactions is the combination of measured Larmor frequencies given by

$$\Delta\omega = \omega_{L,\mathrm{He}} - \frac{\gamma_{\mathrm{He}}}{\gamma_{\mathrm{Xe}}}\,\omega_{L,\mathrm{Xe}}. \tag{5}$$

By that measure, the Zeeman term is eliminated, and thus any dependence on fluctuations and drifts of the applied magnetic field $\Delta\omega$, or its equivalent — the residual phase $\Delta\Phi(t) = \Phi_{\mathrm{He}}(t) - \gamma_{\mathrm{He}}/\gamma_{\mathrm{Xe}} \cdot \Phi_{\mathrm{Xe}}(t)$, is the relevant quantity to be further analyzed in order to trace tiny symmetry violations of the type as mentioned above.

The essential difference, in particular to $^3$He/$^{129}$Xe spin masers used so far, is, that by monitoring the free spin precession, an ultra-high sensitivity can be achieved with a clock being almost completely decoupled from the environment, i.e., no AC-stark shift, no feedback phase jitter, etc. The prerequisite that has to be fulfilled is that the spin-coherence times $T_2^*$ have to reach hours or days. The design and operation of the $^3$He/$^{129}$Xe co-magnetometer have been shown recently [26].

According to the Cramer–Rao Lower Bound (CRLB) [27], the accuracy by which the frequency of a damped sinusoidal signal can be determined is given by

$$\sigma_f \geqslant \frac{\sqrt{12}}{(2\pi)\mathrm{SNR}\sqrt{f_{\mathrm{bw}}}T^{3/2}}\,\sqrt{C(T,T_2^*)}, \tag{6}$$

with SNR denoting the signal-to-noise ratio; $f_{\mathrm{bw}}$ is the bandwidth, and $C(T,T_2^*)$ describes the effect of the exponential damping of the signal amplitude with the transverse relaxation time $T_2^*$. For observation times $T \leqslant T_2^*$, $C(T,T_2^*)$ is of order one. Thus, the sensitivity of a co-located $^3$He/$^{129}$Xe spin clock strongly depends on the observation time $T$. Deviations from the CRLB power-law ($\sim T^{-3/2}$), due to noise sources inherent in the co-magnetometer, have to be tested in Allan standard deviation plots used to identify the power-law model for the phase noise spectrum. We could show, that the noise of our $^3$He/$^{129}$Xe spin clock is the Gaussian distributed at least up to observation times of $T \approx 10000$ s [26] — one essential requirement, the derivation of CRLB is based on.

In typical NMR experiments, the transverse relaxation time $T_2^*$ is of order ms only. Thus, the Fourier limit sets clear limits in the achievable accuracy of frequency measurement. The origin of this relaxation mechanism is the loss of phase coherence of the atoms due to the fluctuating magnetic field seen by the atoms as they diffuse throughout the cell (self-diffusion). Long spin-coherence times $T_2^*$ of macroscopic samples are therefore essential to reach the pHz sensitivity range. At low gas pressures $p$, i.e., the regime of motional narrowing, and at low magnetic fields, the field gradient induced transverse relaxation rate for a spherical spin-sample cell of radius $R$ is given by [28]

$$\frac{1}{T_{2,\mathrm{field}}} \approx \frac{4R^4\gamma^2}{175D}\left(|\boldsymbol{\nabla}B_{1,y}|^2 + |\boldsymbol{\nabla}B_{1,z}|^2 + 2\,|\boldsymbol{\nabla}B_{1,x}|^2\right), \tag{7}$$

$D$ is the diffusion coefficient with $D \sim 1/p$. Since we have $1/T_{2,\mathrm{field}} \sim R^4\,|\nabla B|^2\,p$ and from SNR $\propto p$, it can be inferred that optimum conditions are met at magnetic fields of $\sim 1$ $\mu$T ($f_{\mathrm{He(Xe)}} \approx 10$ Hz) and at gas pressures around 1 mb for a spherical sample cell of radius $R \sim 3{-}5$ cm [26]. Including the longitudinal relaxation time $T_1$, the general expression for the transverse relaxation rate $1/T_2^*$ is $1/T_2^* = 1/T_1 + 1/T_{2,\mathrm{field}}$.

Our experiments were performed at the Berlin Magnetically Shielded Room (BMSR-2) located at the Physikalisch-Technische Bundesanstalt in Berlin. Magnetic fields such as the Earth field and external field disturbances are shielded as effective as nowhere else [29, 30]. According to (7), this shielding together with the reduction of field gradients stemming from the innermost shield is indispensable in order to reach absolute field gradients of order pT/cm across the $^3$He/$^{129}$Xe spin sample necessary to get therefore long spin-coherence times $T_2^*$. In the measurements, a SQUID (Superconducting QUantum Interference Device) vector magnetometer system was used, which has been originally designed for biomagnetic applications inside BMSR-2. The sample cells were placed directly below the Dewar as close as possible to a SQUID sensor, which detects a sinusoidal $B$-field change due to the spin precession of the gas atoms. Inside the $\mu$-metal shielded room, a homogeneous magnetic field of about 300–400 nT was provided by two square coil pairs ($B_x$-coil and $B_y$-coil) which were arranged perpendicular to each other. The use of two coil pairs was chosen in order to manipulate the sample spins, e.g., $\pi/2$ spin-flip.

Characteristic spin precession times $T_2^*$ of up to 110 h were measured. With the obtained measurement sensitivity in the nHz range, it was possible to determine: a) upper limits for the equatorial component of the background field interacting with the spin of the bound neutron [31, 32] (search for the Lorentz violating signatures) and b) new constraints for the monopole–dipole coupling of pseudoscalar particles to the spin of a bound neutron [33–35] (search for spin-dependent short-range interactions). Our new project, the search for a finite electric dipole moment (EDM) of $^{129}$Xe is in progress. Permanent atomic

EDMs would imply a breakdown of both parity and time reversal symmetry and therefore lead to a violation of CP symmetry. Thus searches for atomic EDMs are an unambiguous method to test physics beyond the Standard Model. Our approach is to use co-located $^3$He/$^{129}$Xe spin polarized samples and to measure their coherent spin-precession over time intervals of about 1 day. This way, as previous measurements have shown, we can reach a measurement sensitivity that will improve the present upper limit $d_{\mathrm{Xe}} < 3 \cdot 10^{-27}\ e\cdot$ cm [25] significantly by almost four orders of magnitude (proposed). In the first step, this experiment will be performed at BMSR-2 using our own SQUID gradiometer system as magnetic flux detector for the precessing spins. The applied electric fields will be around 2 kV/cm.

## 3. SUMMARY

A central production facility for hyperpolarized $^3$He based on direct optical pumping of metastable $^3$He atoms combined with a polarization preserving mechanical compression of the gas up to a pressure of several bars has been realized. The Mainz polarizer reaches production rates of several standard liters per hour. Furthermore, all the needed techniques and devices for storage, transport, administration and recovery of spin polarized $^3$He have been developed. The present infrastructure allows numerous applications of polarized $^3$He in both medical research and fundamental science. As an example, recent results with nuclear spin clocks were discussed: $^3$He/$^{129}$Xe clock-comparison experiments, based on the detection of free spin precession of gaseous, nuclear polarized $^3$He and $^{129}$Xe samples with a SQUID as magnetic flux detector are particular attractive to investigate fundamental symmetries in nature. Thanks to the extraordinary long nuclear spin-coherence times of order 100 h, one reaches measurement sensitivity in the nHz range and below. That allows one to trace tiny frequency shifts induced, e.g., by symmetry breaking interactions.

REFERENCES

1. *Colegrove F. D., Schearer L. D., Walters G. K.* // Phys. Rev. 1963. V. 132. P. 2561.
2. *Nacher P. J., Leduc M.* // J. Phys. 1985. V. 46. P. 2057.
3. *Blankleider B., Woloshyn R. M.* // Phys. Rev. C. 1984. V. 29. P. 538.
4. *Krimmer J. et al.* // Nucl. Instr. Meth. A. 2009. V. 611. P. 18.
5. *Krimmer J. et al.* // Nucl. Instr. Meth. A. 2011. V. 648. P. 35.
6. *Heil W. et al.* // Nucl. Instr. Meth. A. 2002. V. 485. P. 551.
7. *Ioffe A., Babcock E., Gutberlet Th.* // J. Phys.: Conf. Ser. 2011. V. 294. P. 011001.

8. *Albert M. S. et al.* // Nature. 1994. V. 370. P. 199.
9. *Ebert M. et al.* // The Lancet. 1996. V. 347. P. 1297.
10. *Leduc M., Nacher P. J.* // CP770, At. Phys. 2005. V. 19. P. 381.
11. *Otten E. W.* // Europhys. News. 2004. V. 35. P. 16.
12. *Terekhov M. et al.* // J. Mag. Res. Imag. 2010. V. 32. P. 887.
13. *Batz M. et al.* // J. Res. Nat. Inst. Stand. Technol. 2005. V. 110. P. 293.
14. *Schmiedeskamp J. et al.* // Eur. Phys. J. D. 2006. V. 38. P. 427.
15. *Hiebel S. et al.* // J. Mag. Res. 2010. V. 204. P. 37.
16. *Güldner M. et al.* // J. Phys.: Conf. Ser. 2011. V. 294. P. 012006.
17. *Salhi Z. et al.* // Mag. Res. Med. 2012. V. 67. P. 1758.
18. *Mrozik C. et al.* // J. Phys.: Conf. Ser. 2011. V. 294. P. 012007.
19. Manufacturing Authorization Ref. No: 2010/128/55/M by the State Office for Social Matters, Youth and Pensions. Rhineland-Palatinate, Germany.
20. *Parker T. E.* // Metrologia. 2010. V. 47. P. 1.
21. *Heil W. et al.* // Proc. of 5th Intern. Symp. on Symmetries in Subatomic Physics (SSP2012).
22. *Kostelecký V. A., Lane C. D.* // Phys. Rev. D. 1999. V. 60. P. 116010.
23. *Moody J. F., Wilczek F.* // Phys. Rev. D. 1984. V. 30. P. 130.
24. *Schmidt Th.* // Z. Physik A. 1937. V. 106. P. 358.
25. *Rosenberry M. A., Chupp T. E.* // Phys. Rev. Lett. 2001. V. 86. P. 22.
26. *Gemmel C. et al.* // Eur. Phys. J. D. 2010. V. 57. P. 303
27. *Kay S. M.* Fundamentals of Statistical Signal Processing: Estimation Theory. V. I. New Jersey: Prentice Hall, 1993.
28. *Cates G. D., Schaefer S. R., Happer W.* // Phys. Rev. A. 1988. V. 37. P. 2887.
29. *Burghoff M. et al.* // Neurology and Clinical Neurophysiol. 2004. V. 67. P. 1.
30. *Schnabel A. et al.* // Ibid. V. 71. P. 1.
31. *Gemmel C. et al.* // Phys. Rev. D. 2010. V. 82. P. 111901.
32. *Allmendinger F. et al.* To be published.
33. *Antoniadis I. et al.* // Comptes Rendus Physique. 2011. V. 12. P. 755.
34. *Burghoff M. et al.* // J. Phys.: Conf. Ser. 2011. V. 295. P. 012017.
35. *Tullney K. et al.* To be published.